Damage production and annealing in ^{28}Si-implanted $CoSi_2$/Si(111) heterostructures

G. Bai[a)] and M.-A. Nicolet
California Institute of Technology, Pasadena, California 91125

(Received 11 July 1991; accepted for publication 4 October 1991)

The damage in epitaxial $CoSi_2$ films 500 nm thick grown on Si(111) produced by room-temperature implantation of 150 keV ^{28}Si were investigated by 2-MeV ^{4}He channeling spectrometry, double-crystal x-ray diffractometry, and electrical resistivity measurements. The damage in the films can be categorized into two types. In lightly (heavily) damaged $CoSi_2$ the damage is in the form of point-like (extended) defects. The resistivity of lightly damaged $CoSi_2$ films rises with the dose of implantation. Electrical defects correlate well with structural ones in lightly damaged films. The resistivity of heavily damaged films flattens off while the structural defects continue to rise with the dose, so that resistivity no longer correlates with structural defects. Upon thermal annealing, lightly damaged films can fully recover structurally and electrically, whereas heavily damaged films do so only electrically. A residual structural damage remains even after annealing at 800 °C for 60 min.

I. INTRODUCTION

Transition-metal silicides are widely used as contacting layers in the metal contacts of Si-based electronic devices.[1,2] The damage produced by the implantation of dopants in a silicide layer and its recovery thus have technological importance. Compared to Si, the metallic silicides are highly resistive to radiation damage.[3–8] Most previous studies have focused on the amorphization of the silicides by implantation and the recrystallization by subsequent thermal annealing.[4–8] An amorphized $CoSi_2$ layer on a crystalline seed recrystallizes in a layer-by-layer manner by solid phase epitaxy.[5–8] Hensel *et al.*[9] studied the effect of ion implantation on carrier transport of $CoSi_2$ films and found that the resistivity increases with dose. We report here some studies on defects production and their annealing in room-temperature ^{28}Si implanted $CoSi_2$ films. The emphasis is on the strain, the damage, and their relationship with the defects in the implanted films. The correlation between structural and electrical defects is also investigated.

II. EXPERIMENTAL PROCEDURES

An epitaxial $CoSi_2$ film 50 nm thick was grown on Si(111) at $\sim$600 °C by molecular beam epitaxy.[10] The samples were implanted at room temperature in vacuum ($\sim 10^{-7}$ Torr) by 150-keV ^{28}Si ions to doses from $5\times10^{13}/cm^2$ to $3\times10^{15}/cm^2$. The beam flux was kept at $\sim 0.2\ \mu A/cm^2$ to minimize the sample heating. The direction of the incident beam was $\sim 7°$ away from the [111] axis to avoid channeling. The maximum damage is located in the Si substrate at a depth of $\sim$150 nm beneath the interface, according to a TRIM88 simulation.[11] The damage in the implanted layers was characterized by 2-MeV ^{4}He ion channeling, Fe Kα_1 x-ray (wavelength $\lambda = 0.1936$ nm) double-crystal diffraction, and electrical resistivity measurements.

The implanted samples were annealed afterwards in vacuum ($\sim 5\times10^{-7}$ Torr) at 250–800 °C for 60 min and the damage recovery was monitored.

III. RESULTS

A. MeV ^{4}He channeling spectrometry

2-MeV ^{4}He[111] axial channeling with a glancing exit angle (82°) was used to measure the damage in the implanted layers. The spectra of the implanted samples show that the channeling yields of both the film and the substrate rise with the dose (Fig. 1). For a given dose, the damage level in the $CoSi_2$ film is much smaller than that in the Si substrate, meaning that $CoSi_2$ is more radiation resistant than Si. The high radiation resistance of $CoSi_2$ agrees with the results of room-temperature implanted Pd_2Si and $NiSi_2$,[3,4] and is consistent with the metallic nature of these silicides.

The damage build up in the Si substrate as a function of the dose is very similar to that observed in self-implanted Si samples.[12] There exist three distinct damage regimes (see Fig. 1). The damage rises slowly as the dose increases from $5\times10^{13}/cm^2$ to $2\times10^{14}/cm^2$ (regime I), and then rapidly rises to the level of an amorphous Si at $5\times10^{14}/cm^2$ (regime II). As the dose increases further, the maximum damage level saturates, and the damage region widens (regime III).

The damage in the $CoSi_2$ film builds up very differently with dose. Below $2\times10^{14}/cm^2$ the channeling yield of the film is the same as that of the as-grown one ($\sim$5%). The channeling yield increases to $\sim$9% at $5\times10^{14}/cm^2$, and rises to $\sim$56% at $3\times10^{15}/cm^2$ (Fig. 1). Maex *et al.*[8] found that the channeling yield of $CoSi_2$ films implanted at room temperature by 200-keV ^{28}Si to $2\times10^{15}/cm^2$ is $\sim$50%, in good agreement with our results. They also observed that

[a)]Current address: Intel Corp., 3065 Bowers Ave., SC1-03. Santa Clara, CA 95052-8126.

 0021-8979/92/140670-06$04.00 © 1992 American Institute of Physics

Downloaded 22 Dec 2005 to 131.215.225.9. Redistribution subject to AIP license or copyright, see http://jap.aip.org/jap/copyright.jsp

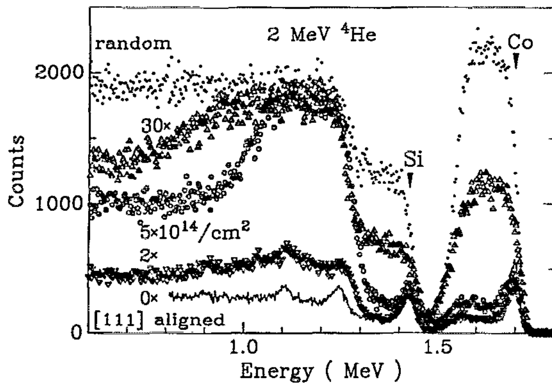

FIG. 1. 2-MeV ^{4}He backscattering spectra with a beam incident along a random (●) and a [111] axial channel orientation of the as-grown epitaxial $CoSi_2$ (50 nm) on Si(111) (solid line) and of the samples implanted at room temperature with 150-keV ^{28}Si to doses of $2\times(\nabla)$, $5\times(\bigcirc)$, $30\times10^{14}/cm^2$ (Δ). The detected ^{4}He particles exit at an angle of 82° from the line of the incident beam.

the damage in $CoSi_2$ is sensitive to the implantation temperature, as it is in Si.[13] Hewett *et al.*[5] demonstrated that $CoSi_2$ can be amorphized by 40–200-keV ^{28}Si implantation to $\sim2\times10^{15}/cm^2$ at liquid-nitrogen temperature.[5–8]

We apply the procedure outlined in Ref. 12 to estimate the defect concentration at a depth x, $c_D(x)$ $(0\leqslant c_D\leqslant1)$, in the implanted $CoSi_2$ film from the channeling measurements. To simplify the analysis, we assume that the fraction of displaced Si atoms in the film is the same as that of displaced Co atoms. The dechanneling factor, $\gamma_D(x)$, is obtained directly from the channeling spectra,[12]

$$\gamma_D(x)\equiv\frac{\chi_D(x)-\chi_V(x)}{1-\chi_V(x)}. \tag{1}$$

where $\chi_D(\chi_V)$ is the channeling yield of the damaged (virgin) sample normalized to the random yield. The defect concentration profile $c_D(x)$ can be extracted from the equation,[12]

$$\gamma_D(x)=P_D(x)+[1-P_D(x)]c_D(x). \tag{2}$$

$P_D(x)$is the dechanneling probability at a depth x,[12]

$$P_D(x)=\int_0^x n\sigma_D c_D(x')dx', \tag{3}$$

where n is the atomic density of $CoSi_2$, and σ_D is the average dechanneling cross section of Si and Co atoms. TRIM88 simulation shows that the damage is roughly a constant through the entire film. The channeling spectra of Fig. 1 suggest the same conclusion. We therefore assume that c_D is depth-independent in the film, and Eq. (3) becomes

$$P_D(x)=(n\sigma_D x)c_D(x). \tag{4}$$

We compute γ_D from the minimum channeling yield of the Co signal at the energy immediately beneath the surface peak ($\sim$1.65 MeV in Fig. 1). The corresponding depth is $x\approx10$ nm. Substituting the appropriate numbers into Eq. (4), and assuming $\sigma_D<10^{-18}/cm^2$ (see Ref. 12), one obtains

$$P_D<0.05c_D.$$

P_D is small compared to c_D, and we therefore neglect the second term in Eq. (2) and have

$$c_D\approx\gamma_D. \tag{5}$$

The defect concentration c_D in the $CoSi_2$ films, extracted from the channeling data according to Eq. (5), is plotted as a function of the implantation dose in Fig. 2 (●). c_D is undetectable ($\leqslant1\%$) after the implantation to $2\times10^{14}/cm^2$, and then increases monotonically with the dose.

For comparison, we also computed by a TRIM88 simulation[11] the concentration of Frenkel pairs directly produced by the implantation of 150-keV ^{28}Si in an amorphous matrix composed of a 50-nm-thick $CoSi_2$ on Si (dashed line in Fig. 1). A displacement threshold energy of 15 eV and a binding energy of 1 eV were assumed. The measured damage is only a small fraction of that initially produced, meaning that the majority of the Frenkel pairs anneal out at room temperature during and after implantation. This observation leads us to attribute the high radiation resistance of $CoSi_2$ to its high defect recombination rate, probably resulting from the higher mobility of point defects in $CoSi_2$ than in Si.

Upon post-thermal annealing, the damage in the Si substrates and $CoSi_2$ films decreases gradually. The annealing characteristics of the damaged Si substrate is similar to that of implanted bulk Si.[12] Different damage regimes have different recovery stages. The higher the damage, the higher the annealing temperature becomes. At low damage levels ($\phi\leqslant2\times10^{14}/cm^2$, regime I) the channeling yield decreases as the annealing temperature rises. The dominant process is probably the recombination of point-like defects. At high damage levels near the amorphization threshold ($\phi=5\times10^{14}/cm^2$, regime II), the channeling spectrum does not change after 60-min isochronal annealing at 250 °C. The channeling yield decreases after 400 °C annealing, and becomes the same as that of the as-grown sample after 600 °C annealing. The channeling spectrum of the amorphized samples ($\phi\geqslant10^{15}/cm^2$, regime III) does not change after 400 °C annealing. In that case, appreciable solid phase epitaxial growth occurs after annealing at 600 °C. However, the channeling yield is very high ($\sim$50%) and remains that high after 800 °C annealing. A high density of extended defects (e.g., dislocation loops, microtwins) is likely present.

Qualitatively, the annealing features of the $CoSi_2$ films are simpler than those of the Si substrate, since the film is not amorphized after implantation to the highest dose of $3\times10^{15}/cm^2$ (see Fig. 1). The channeling yields of the implanted films decrease with increasing annealing temperature. The defect concentration in the film after annealing at various temperatures, extracted from the channeling yield according to Eq. (5), is shown in Fig. 2. The films implanted to a dose of $\leqslant5\times10^{14}/cm^2$ completely recover,

Downloaded 22 Dec 2005 to 131.215.225.9. Redistribution subject to AIP license or copyright, see http://jap.aip.org/jap/copyright.jsp

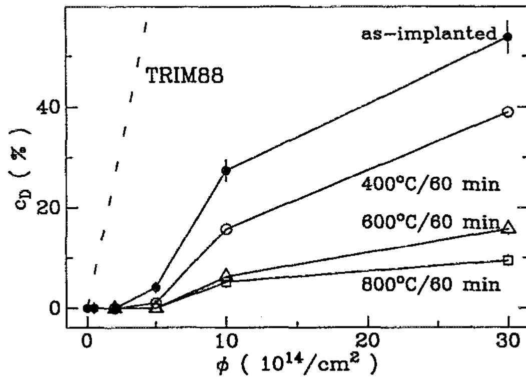

FIG. 2. Defect concentration in the $CoSi_2$ films extracted from the channeling yields of Fig. 1 vs the ^{28}Si dose, for the as-implanted samples (●), and those annealed for 60 min at 400 °C (○), 600 °C(△), 800 °C (square). The Frenkel pair concentration as a function of the dose, predicted from a TRIM88 simulation, is also shown (dashed line).

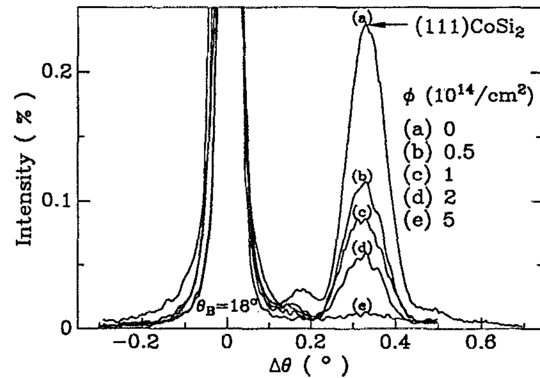

FIG. 3. Rocking curves for Fe $K\alpha_1$ x-rays diffracted from symmetrical (111) planes (a) of as-grown $CoSi_2$/Si(111) and of the samples implanted to doses of (b) 0.5×, (c) 1×, (d) 2×, (e) 5×10^{14}/cm^2. The Bragg peak from the bulk Si substrate is at $\theta_B = 18°$.-

while those implanted to doses $\geqslant 10^{15}$/cm^2 do not. We believe that the nonzero defect concentration ($\sim$10%, Fig. 2) after annealing is indicative of the presence of residual defects that are extended, rather than a measure of the concentration of point defects. These observations suggest that there exist two distinct damage structures in ion implanted $CoSi_2$. The defects in the lightly damaged films ($\phi < 5\times10^{14}$/cm^2) are simple and anneal out completely upon thermal processing. The defects in the heavily damaged films ($\phi > 10^{15}$/cm^2) are complex and the recovery is incomplete. We note that the incomplete recovery of the film coincides with that of the Si substrate.

B. X-ray double-crystal diffractometry

A heterostructure differs from a bulk crystal in that there exists intrinsic strain in an as-grown heterostructure. Implantation produces defects, which induce additional strain in the heteroepitaxial film. We use x-ray double-crystal diffraction to monitor the strain change in the $CoSi_2$ film as a result of the implantation. Figure 3 shows a set of x-ray rocking curves diffracted from the (111) symmetrical plane of the $CoSi_2$/Si(111) samples implanted to a dose of (a) 0×, (b) 0.5 ×, (c) 1×, (d) 2×, (e) 5×10^{14}/cm^2.

Based on previous studies on implantation in Si(100),[12] we expect that the damage in the Si substrate induces positive strain, and that an additional diffraction peak will appear on the low-angle side of the bulk Si peak at $\theta_B = 18°$ in Fig. 3. Implantation to $\leqslant 2\times10^{14}$/cm^2 produces low damage (regime I) in the Si substrate, and induces a small perpendicular strain of $\leqslant$0.1% there (see Ref. 12). The shift in the angular position for the (111) diffraction peak of the implanted layer is correspondingly small ($\leqslant$0.02°) and undetectable because it lies within the main peak (see Fig. 3). Implantation to $\geqslant 5\times10^{14}$/cm^2 produces high damage (regime II) or a continuous amorphous layer (regime III)[12] the corresponding diffraction peak then becomes weak and is buried in the background intensity ($\sim$0.003%, see Fig. 3).

The peak intensity of x-rays diffracted from the $CoSi_2$ (111) planes decreases with increasing dose (Fig. 3). After implantation to a dose of 2×10^{14}/cm^2, the intensity drops to $\sim\frac{1}{4}$ of that of the as-grown film, unlike the channeling yield which is the same as that of the as-grown sample (Figs. 1 and 2). This fact demonstrates that x-ray diffraction is much more sensitive to low defect concentrations than channeling. The x-ray intensity from the $CoSi_2$ layer of the sample implanted to a dose of $\geqslant 10^{15}$/cm^2 drops below the background ($\sim$0.003%) and hence becomes unmeasurable. The defect concentration extracted from the channeling yield of that same sample is only about 27%. A comparison of the channeling spectra (Fig. 1) and x-ray rocking curves (Fig. 3) of the implanted $CoSi_2$ films clearly illustrates that channeling is insensitive to low damage ($c_D \leqslant 1\%$), while the x-ray diffraction from the highly damaged films ($c_D \geqslant 27\%$) becomes unmeasurable. These two techniques are therefore complementary and together provide a good picture of damage production by ion implantation in $CoSi_2$.

In the following, we will analyze quantitatively the x-ray rocking curves diffracted from the lightly damaged $CoSi_2$ films ($\sigma \leqslant 5\times10^{14}$/cm^2). The angular position of the (111) diffraction peak does not change with the dose, which means that the perpendicular star in $c^\perp$ in the films is a constant, $\sim -1.76\%$, within the experimental sensitivity ($\sim$0.08%). In other words, the upper limit in the difference of the magnitude of the strain between the implanted and as-grown films, $|\Delta\epsilon^\perp|$, is $\sim$0.08%. The defect concentration c_D in the corresponding films ranges from $\leqslant$1% to $\sim$4% (● in Fig. 2). These results imply that in the lightly damaged $CoSi_2$ films, one has

$$|\Delta\epsilon^\perp| \leqslant 0.02 c_D. \qquad (6)$$

We were unable to measure the parallel strain in our $CoSi_2$ films because they are B type.[14] We know, however, that the interfacial misfit dislocations do not shear at room

Downloaded 22 Dec 2005 to 131.215.225.9. Redistribution subject to AIP license or copyright, see http://jap.aip.org/jap/copyright.jsp

temperature.[15] It is therefore reasonable to assume that the parallel strain of the film remains unchanged upon the implantation, i.e., $\Delta\epsilon^{\parallel}=0$. It then follows (see Ref. 12) that the lattice dilatation, $\Delta a/a$, of the $CoSi_2$ induced by the defects is

$$\left|\frac{\Delta a}{a}\right|=\left(\frac{1-\nu}{1+\nu}\right)|\Delta\epsilon^{\perp}|\leqslant 0.01c_D, \tag{7}$$

where a is the lattice constant of the as-grown $CoSi_2$ film, and ν is Poisson's ratio of $CoSi_2$ ($=\frac{1}{3}$, see Ref. 15). The coefficient relating $|\Delta a/a|$ to c_D for ion implanted $CoSi_2$ is $\leqslant 0.01$. This value is about two orders of magnitude smaller than that for vacancy-interstitial pairs in fcc crystals (~ 1),[16,17] but is about the same as that for ion implanted Si($\sim$0.007, see Ref. 12). This fact suggests that the defects in lightly damaged $CoSi_2$ films consist of defect clusters, not of single vacancies and interstitials. This result is consistent with our previous assertion that point defects in $CoSi_2$ are mobile at room temperature.

The full width at half maximum of all diffraction peaks that are strong enough to be detected (films implanted to $\leqslant 5\times 10^{14}/cm^2$) is an invariant (see Fig. 3), independent of the damage induced by ion implantation. The peak broadening in the present case is due to the finite film thickness. This result implies that the x-ray diffraction from the lightly damaged film is highly coherent, and suggests that the damage in the implanted film consists mainly of randomly distributed defect clusters. The x-ray diffraction from a lightly damaged $CoSi_2$ film can therefore be modeled by a static Debey–Waller factor, which does not change the peak width but only decreases the intensity.[18] The ratio of the peak intensity from the implanted film, I_D, to that from the as-grown one, I_V, equals,[18]

$$\frac{I_D}{I_V}=\exp\left(-\frac{16\pi^2}{3}u_D^2\frac{\sin^2\theta_B}{\lambda^2}\right), \tag{8}$$

where u_D is the mean square root of the atomic displacement caused by the point-like defects in the implanted film. For Fe K_{a_1} x rays diffracted from CoSi(111) planes, Eq. (8) results in

$$u_D=0.085\sqrt{\ln\frac{I_V}{I_D}}\ (\text{nm}). \tag{9}$$

The displacement u_D in the lightly damaged $CoSi_2$ film, extracted from the measured intensities in Fig. 3 according to Eq. (9), rapidly rises to $\sim$0.06 nm after implantation to $5\times 10^{13}/cm^2$ and then increases linearly with dose (● in Fig. 4).

Upon 30-min isochronal annealing at 250, 400, 600, and 800 °C in high vacuum, both the angular position and the width of the x-ray diffraction peak from the lightly damaged $CoSi_2$ films ($c_D\leqslant 4\%$) remain unchanged. This means that within the experimental sensitivity, the strain of the $CoSi_2$ films does not change, $\epsilon^{\perp}\sim -1.76\%$ at room temperature. The presence of a small defect concentration in the metastable $CoSi_2$ film (a 50-nm-thick $CoSi_2$ film on Si(111) at an equilibrium state has $\epsilon^{\perp}\sim -1.23\%$ at room temperature) during thermal annealing evidently does not

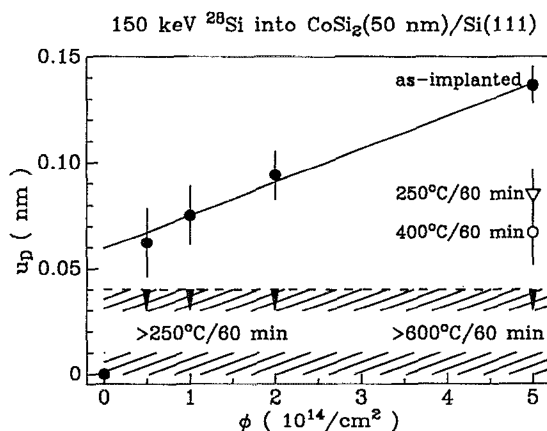

FIG. 4. Static atomic displacement induced by the defects in the lightly damaged $CoSi_2$ films vs the ^{28}Si dose, for the as-implanted samples (●), and for those annealed in vacuum for 60 min at 250 °C (∇) and 400 °C(○). The shaded area represents the range of experimental uncertainty in estimating the displacement of a perfect $CoSi_2$ film.

enhance the strain relaxation. The x-ray peak intensity rises with increasing temperature. For the films implanted up to $2\times 10^{14}/cm^2$, the intensity after 250 °C is the same as that of the as-grown film within the experimental uncertainty ($\sim$20%). The uncertainty in the intensity measurements causes a corresponding uncertainty in the estimation of the atomic displacement extracted according to Eq. (9),

$$\frac{\delta u_D/u_D}{\sqrt{(\delta I_D/I_D)^2+(\delta I_V/I_V)^2}}=\frac{0.5}{\ln(I_V/I_D)}. \tag{10}$$

This relationship shows that u_D of the film with an intensity close to that of I_V has a large percentage error. For a relative error of the x-ray intensity of $\sim$20%, the error of u_D is about 0.04 nm. Stated differently, a measured displacement of 0–0.04 nm all corresponds to a perfect $CoSi_2$ film. The displacement extracted for the films implanted to $\leqslant 2\times 10^{14}/cm^2$ after all annealings is $\leqslant$0.04 nm (Fig. 4). This suggests that these films recover completely after all annealings. The displacement of the film implanted to $5\times 10^{14}/cm^2$ decreases with increasing annealing temperature, and becomes indistinguishable from that of the as-grown film after 600 °C annealing (Fig. 4).

The heavily damaged $CoSi_2$ films ($\phi\geqslant 10^{15}/cm^2$) have very different annealing characteristics. Upon thermal annealing, the x-ray peak intensity rises out of the background ($\sim$0.003%) and becomes remeasurable. The peak position is about the same as that of the as-grown film, meaning that the strain of the heavily damaged films does not change after annealing. However, the peak is much broader and weaker than that of the as-grown film, even after 800 °C. This result signifies that the strain in the annealed films is very inhomogeneous, and indicates the presence of extended defects. These results correlate well with those obtained from channeling measurements.

Downloaded 22 Dec 2005 to 131.215.225.9. Redistribution subject to AIP license or copyright, see http://jap.aip.org/jap/copyright.jsp

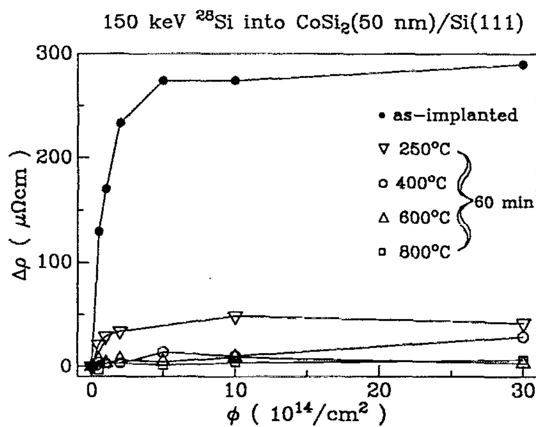

FIG. 5. Room-temperature resistivity difference between the as-grown $CoSi_2$ film (~16 μΩ cm) and the implanted ones vs the dose, for the as-implanted sample (●), and for those annealed in vacuum for 60 min at 250 °C (∇), 400 °C (○), 600 °C (△), 800 °C (square).

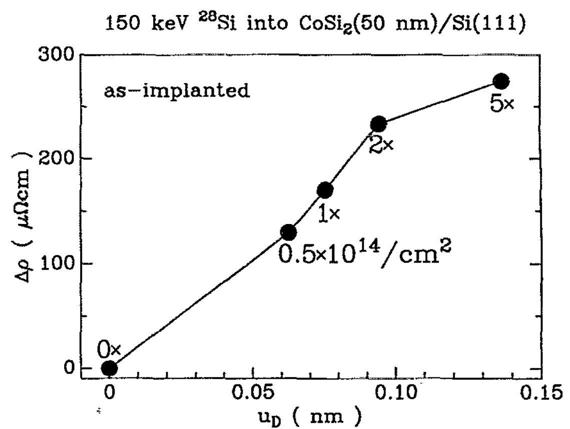

FIG. 6. Resistivity difference vs the static displacement for the lightly damaged $CoSi_2$ films ($\phi \leq 5\times10^{14}/cm^2$). The approximately linear relationship indicates a good correlation between the concentration of the carrier scatterers and the structural defects in such films.

C. Electrical resistivity

We also measured the resistivity in the implanted film with a four-point probe to monitor the evolution of defects. The sheet resistance of the selected samples was also measured by the van der Pauw method, and agreed with that of the four-point probe measurements. Current-voltage measurements show that the vertical resistance across the silicide-silicon interface is always much greater than the sheet resistance of the silicide film for all samples, meaning that the film is practically insulated from the substrate. The resistivity was extracted from the sheet resistance with the film thickness of 50 nm obtained from backscattering measurements. The measured resistivity of the $CoSi_2$ films rises with the dose of ion implantation. This is similar to what is observed for other implanted metallic silicides,[19] but is opposite to what is found for implanted semiconducting silicides ($ReSi_2$ from Ref. 20, $CrSi_2$ from Ref. 21). The resistivity of $CoSi_2$ films increases from ~16 μΩ cm for the as-grown sample to ~300 μΩ cm for the sample implanted to $5\times10^{14}/cm^2$ and flattens off up to $3\times10^{15}/cm^2$ (Fig. 5).

The resistivity, ρ, of metals can be decomposed into two terms according to Matthiessen's rule,

$$\rho(T)=\rho_L(T)+\rho_D, \quad (11)$$

where ρ_L is the lattice (Bloch–Gruneisen) contribution, and ρ_D results from carrier scattering by defects at 0 K. Hensel *et al.*[9] measured the resistivity of $CoSi_2$ films bombarded with 2-MeV ^{4}He at 4–300 K and found good agreement with Eq. (11). These authors also established that the resistivity of samples implanted to different doses has a similar temperature dependence, meaning that the lattice contribution $\rho_L(T)$ is the same regardless of the damage (so long as the film is not amorphized to cause localization of carriers). The difference of ρ between the bombarded and the as-grown films, $\Delta\rho$, hence equals $\Delta\rho_D$, the resistivity contribution from radiation-induced defects. In an as-grown $CoSi_2$ film, ρ_D is ~2 μΩ cm.[9] Hensel *et al.*[9] discovered that $\Delta\rho_D$ rises approximately linearly with dose till ~100 μΩ cm and then flattens off with further dose increase. The resistivity jumps abruptly to ~1000 μΩ cm once the $CoSi_2$ is amorphized, and remains constant thereafter. This is also the resistivity of amorphized $ReSi_2$ films (~1200 μΩ cm).[20] The common value of the resistivity of amorphized metallic and semiconducting silicides suggests that the conduction in such an amorphous state is dominated by hopping of localized charge carriers.

We used the van der Pauw method to measure the resistivity of the $CoSi_2$ film for selected samples at 130–300 K. The temperature dependence of the resistivity agrees with the prediction of Eq. (11), and that reported by Hensel.[9] We assume in the following that the resistivity difference $\Delta\rho$ between the implanted and the as-grown $CoSi_2$ films equals that induced by the implantation $\Delta\rho_D$ for all our samples ($CoSi_2$ is not amorphized). $\Delta\rho_D$ increases with dose to ~280 μΩ cm at $5\times10^{14}/cm^2$ and flattens off up to $3\times10^{15}/cm^2$ (● in Fig. 5). The different resistivity at plateau between our result and that of Hensel *et al.*[9] (280 vs 100 μΩ cm) is probably due to the different implantation conditions (230-keV ^{28}Si vs 2-MeV ^{4}He) that produce different microstructures of defects in the implanted $CoSi_2$ film.

The resistivity from carrier scattering by point-like defects is proportional to the density of scatterers. The initial rise of $\Delta\rho_D$ in lightly damaged films ($\phi \leq 5\times10^{14}$) suggests that the implantation produces point-like defects which build up with increasing dose.[9] This conclusion is very similar to that drawn from x-ray diffraction results (see previous discussion). Figure 6 plots the resistivity caused by defects scattering as a function of the atomic displacement induced by defects in lightly damaged $CoSi_2$ film ($\phi \leq 5\times10^{14}/cm^2$, see Figs. 2, 4, and 5). The plot shows a good correlation between these two indicators of the defect concentration in the $CoSi_2$ films. In heavily damaged $CoSi_2$ films, with dose from $10^{15}/cm^2$ to $3\times10^{15}/cm^2$, $\Delta\rho_D$ is roughly a constant (~280 μΩ cm, Fig. 5), while the defect concentration c_D extracted from the channeling yields increases from ~27% to ~54% (● in Fig. 2). This sug-

Downloaded 22 Dec 2005 to 131.215.225.9. Redistribution subject to AIP license or copyright, see http://jap.aip.org/jap/copyright.jsp

gests that the flat $\Delta\rho_D$ is probably indicative of some agglomeration of defects in heavily damaged films,[9] in agreement with the results from annealing studies by channeling and x-ray diffraction.

The resistivity of the $CoSi_2$ films of all samples decreases drastically after 250 °C (∇ in Fig. 5), and becomes about the same as that of the as-grown sample after 600 °C (Δ in Fig. 5). The decrease of the resistivity of lightly damaged films ($\phi < 5\times10^{14}/cm^2$) after annealing correlates well with the recovery of structural defects probed by channeling and x-ray diffraction measurements. For highly damaged films ($\phi > 10^{15}/cm^2$), the structural recovery after annealing is incomplete, with a channeling yield of $\sim 10\%$ (greater than that of the as-implanted films to a dose $\leqslant 5\times10^{14}/cm^2$), and with a broad x-ray diffraction peak that suggests the existence of extended defects in these annealed films. Yet the resistivity of such films is about the same as those of the structurally perfect ones, much less than that of the as-implanted films of any dose. Apparently the residual extended defects that still exist in the highly damaged films after annealing are ineffective scattering centers for the carrier transport.

IV. CONCLUSION

In summary, we demonstrate that MeV ion channeling is well suited to characterize heavily damaged $CoSi_2$ films ($c_D > 1\%$) while x-ray diffraction does best for lightly damaged ones. Resistivity is a relevant indicator of the damage over the entire range. A linear relationship exists between the structural and the electrically active defects in lightly damaged films. Such a relationship is absent in heavily damaged $CoSi_2$, where the resistivity flattens but the defect concentration increases further with dose. Lightly damaged films recover completely upon thermal annealing. Heavily damaged films also recover their original resistivity after annealing, but extended defects (e.g., dislocation loops and microtwins) that are ineffective for carrier scattering subsist.

ACKNOWLEDGMENTS

The authors thank Dr. Y. C. Kao and Dr. K. L. Wang at UCLA for providing the as-grown $CoSi_2$/Si(111) samples. This work is supported in part by the Semiconductor Research Corporation under the contract No. 100-SJ-90, and by the National Science Foundation under the grant No. DMR-8811795. The authors gratefully acknowledge this support.

[1] M-A. Nicolet and S. S. Lau, in *VLSI Electronics*, Vol. 6, edited by N. G. Einspruch and G. B. Larrabee (Academic, New York, 1983), p. 330.
[2] S. P. Murarka, *Silicides for VLSI Applications* (Academic, New York, 1983).
[3] H. Ishiwara, K. Hikosaka, and S. Furukawa, Appl. Phys. Lett. **32**, 23 (1978).
[4] M. Mäenpää, L. S. Hung, M-A. Nicolet, D.K. Sadana, and S. S. Lau, Thin Solid Films **87**, 277 (1982).
[5] C. A. Hewett, I. Suni, S. S. Lau, L. S. Hung, and D. M. Scott, Mater. Res. Soc. Symp. Proc. **27**, 145 (1984).
[6] C. A. Hewett, S. S. Lau, I. Suni, and L. S. Hung, J. Appl. Phys. **57**, 1089 (1985).
[7] M. C. Ridgway, R. G. Elliman, R. P. Thornton, and J. S. Williams, Appl. Phys. Lett. **56**, 1992 (1990).
[8] K. Maex, A. E. White, K. T. Short, Y. F. Hsieh, R. Hull, J. W. Osenbach, and H. C. Praefcke, J. Appl. Phys. **68**, 5641 (1990).
[9] J. C. Hensel, R. T. Tung, J. M. Poate, and F. C. Unterwald, Nucl. Instrum. Meth. B **7/8**, 409 (1985).
[10] Y. C. Kao, K. L. Wang, E. de Fresart, R. Hull, G. Bai, D. N. Jamieson, and M-A. Nicolet, J. Vac. Sci. Technol. B **6**, 745 (1987).
[11] J. P. Biersack and L. G. Haggmark, Nucl. Instrum. Meth. **174**, 257 (1980).
[12] G. Bai and M-A. Nicolet, J. Appl. Phys. **70**, 649 (1991).
[13] J. F. Gibbons, Proc. IEEE **6**, 1062 (1972).
[14] R. T. Tung, J. C. Bean, J. M. Gibson, J. M. Poate, and D. C. Jacobson, Appl. Phys. Lett. **40**, 684 (1982).
[15] G. Bai, M-A. Nicolet, and T. Vreeland, Jr., J. Appl. Phys. **69**, 6451 (1991).
[16] L. Tewordt, Phys. Rev. **109**, 61 (1958).
[17] H. G. Haubold and D. Martinsen, J. Nucl. Mater. **69/70**, 644 (1978).
[18] B. E. Warren, *X-Ray Diffraction* (Dover, New York, 1990).
[19] B-Y. Tsaur and C. H. Anderson, Jr., J. Appl. Phys. **53**, 94 (1982).
[20] K. H. Kim, G. Bai, M-A. Nicolet, J. E. Mahan, and K. M. Geib, Appl. Phys. Lett. **58**, 1884 (1991).
[21] T. C. Banwell, X. A. Zhao, and M-A. Nicolet, J. Appl. Phys. **59**, 3077 (1986).

Downloaded 22 Dec 2005 to 131.215.225.9. Redistribution subject to AIP license or copyright, see http://jap.aip.org/jap/copyright.jsp